

Fisher Space Systems, LLC

Space Track Launch System Proof of Concept System

by
Jerry F. Fisher

1.0 Introduction

The Space Track Launch System (STLS) is a two stage launch system. The first stage is a tall tower with rotating ribbons (Fisher, J.F., 2011). The tower (figure 1) is from 100-150 km in height. At the top of the tower, there is a rotating truss which supports four ribbons (two ribbons from each end of the truss) made of high strength fiber composites. Counterweights (CW) (Fisher, J.F., 2010) are attached to the end of each ribbon.

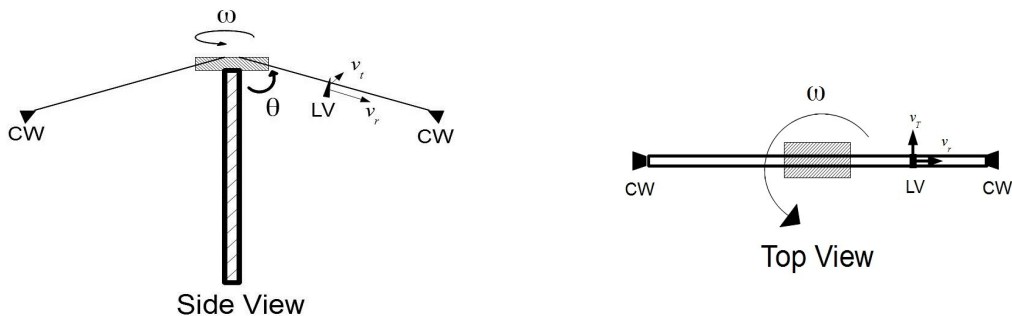


Figure 1. Space Track Launch System

The second stage is a liquid fueled launch vehicle (LV) designed to launch from the STLS (Fisher, J.F., 2009). The launch vehicle attaches to an ejector which is attached to an overcarriage (Fisher, J.F., 2010). The overcarriage has four tapered wheels which rest on top of the ribbon. The overcarriage and launch vehicle travel down the ribbon and are accelerated by the centrifugal force resulting from the distance from the axis of rotation and by the contact force (Coriolis force) provided by the rotating ribbon. At a predetermined point along the ribbon, the ejector fires and the launch vehicle detaches from the overcarriage and ribbon. The liquid propellant rocket engines ignite and the second stage proceeds into orbit. The overcarriage returns to the launch site to be refurbished and reused.

This paper discusses the proof of concept system. The proof of concept system will be a 25 km tall sub-scale model of a fully operational first generation system. The proof of concept system will demonstrate the launch of a second stage suborbital launch vehicle with separation from an overcarriage on a rotating ribbon.

At launch, a shock wave is produced in the ribbon. If left unchecked, the shock wave will severely damage if not destroy the ribbon and tower. By using the overcarriage and

Fisher Space Systems, LLC

counterweight, the proof of concept system will demonstrate the mitigation of the shock wave in the ribbon.

While restoring rotational kinetic energy to the ribbon, torque is produced by the high temperature superconducting motors. The torque is fully eliminated by the torque buffer. The proof of concept system will demonstrate torque buffering while restoring rotational kinetic energy to the ribbon.

While rotating, the ribbons and counterweights produce an unbalanced force directed southward which will cause the tower to precess. The proof of concept system will demonstrate gyroscopic and pressure stabilization of the unbalanced force and greatly reduce tower precession.

Tower loads for the second generation system are estimated to be 3,000 metric tons. Tower loads for the first generation system are estimated to be 800 metric tons. The proof of concept system will have an estimated peak tower load of 600 metric tons. Tower loads of these magnitudes at the required altitudes can be met with inflated multi-beam technology. The proof of concept system will demonstrate the viability of using inflated multi-beams for the all electric first stage of the Space Track Launch System.

Section 2.0 of the paper estimates the tower load for the proof of concept system. The tower load consist of the ribbon, counterweight, launch vehicle, overcarriage, truss, gears, motors, guy wires, and transfer station. Section 3.0 of the paper discusses the support tower. The support tower consist of the torque buffer, guy wires, interface rings, and inflated multi-beams. Section 4.0 is the conclusion.

2.0 Tower Load (Mass Estimates)

The tower load consist of the ribbon, counterweight, launch vehicle, overcarriage, truss, gears, motors, guy wires, and transfer station. As discussed below and summarized in table IV, the estimated mass is 383 metric tons which represents a static tower load of approximately 3.8×10^6 N. While torque buffering and pressure stabilizing, the guy wires produce an additional dynamic load of 2.1×10^6 N. As such, the peak load on the first layer of beams is an estimated 5.9×10^6 N.

The peak tower load occurs during torque buffering and pressure stabilization of the tower. Torque is produced when the high temperature superconducting electric motors start the truss, ribbon, and counterweight rotating and when rotational kinetic energy is restored after launch. Pressure stabilization is required to compensate for the unbalance load during rotation. To prevent overloading the tower, torque buffering and pressure stabilization do not occur at the same time but are 90° out of phase. A more detailed discussion of the tower load follows in the subsections below.

2.a. Ribbon and Counterweight

At 25 km altitude, atmospheric heating limits the length of the ribbon to about 2 km.

Fisher Space Systems, LLC

Fortunately, for the proof of concept system, the second stage launch vehicle is suborbital and therefore, launch velocity is not a driving factor. The driving factor is getting the second stage and overcarriage far enough down the ribbon for a safe launch and to prove the concept. As discussed below, the power into the ribbon is a result of aerodynamic drag, solar radiation, and the albedo of the Earth. The power out of the ribbon is mainly due to convection and radiation.

The purpose of the counterweight (CW) is to maintain the proper angle of attack for the ribbon and absorb some of the shock of launch. As such, the CW will be designed as a fuselage with a tail boom and elevator. The mass of the CW has an overall impact on the dynamics of the ribbon as well as the ribbon mass. As discussed below, the estimated mass of the ribbon and counterweight is approximately 29 tons.

2.a.1. Ribbon Length

Aerodynamic heating, solar radiation, and Earth's albedo limit the length of the ribbon to about 2 km. The last 10 m segment of the ribbon (i.e. the ribbon segment connected to the CW) experiences the greatest temperature. This is due to its distance from the axis of rotation and therefore, its higher velocity relative to the other ribbon segments.

The temperature of the last segment of the ribbon is determined by using the conservation of energy and the heat transfer equations (Incropera, F.F. and DeWitt, D.P., 1985). The conservation of energy requires that the power going into the ribbon equal the power coming out. The major source of power into the ribbon segment is the sum of that produced by aerodynamic heating, solar radiation, and the albedo of the Earth.

The power into the last 10 m ribbon segment due to aerodynamic heating of the segment is given by,

$$P_{aero} = F_d v = 0.5 C_d \rho v^3 A$$

where C_d is the coefficient of drag, ρ is the density of the atmosphere, v is the velocity of the ribbon segment, and A is the surface area of the ribbon segment.

The coefficient of drag is an empirical number for most airfoils and is determined by experiment which is beyond the scope of this paper. However, a working value of .01 can be used and is derived by assuming a thin flat plate airfoil in a high altitude high velocity simulation such as NASA's FoilSim III Applet (FoilSim, 2012). The input parameters are shown in the references. From the standard atmosphere model, the density of the atmosphere at 25 km is approximately $4.1 \times 10^{-2} \text{ kg/m}^3$. The velocity of the ribbon segment is about 315 m/s and the surface area is 10 m^2 . From the equation above, the power into the ribbon segment is about 64.1 kW.

The power into the ribbon segment due to direct solar radiation is given by (Carroll, J.A., 1985),

Fisher Space Systems, LLC

$$P_{solar} = 1368 \sigma_s A$$

where σ_s is equal to 0.4 for Kevlar (Carroll, J.A., 1985) and A is equal to 10 m². From the above equation, the power into the ribbon due to solar radiation is about 5.5 kW.

The power into the ribbon segment due to the albedo of the Earth is given by (Carroll, J.A., 1985),

$$P_{albedo} = 506 \sigma_s A$$

which is equal to about 2.0 kW. Therefore, the total power into the last 10 m segment of ribbon is approximately 71.6 kW.

The power out of the ribbon segment is due to conduction, convection, and radiation. The power out of the ribbon segment through conduction is given by,

$$P_{cond} = \frac{k}{L} (T_1 - T_2) A_x = \frac{k}{L} (\Delta T) A_x$$

where k is the thermal conductivity, L is the length of the ribbon segment, A_x is the cross sectional area of the ribbon segment, and $T_1 - T_2 = \Delta T$ assumes a linear temperature gradient. The thermal conductivity of Kevlar 49 is 0.04 W/m-K (Kevlar, 2012) and the cross sectional area of the ribbon segment is on the order of 10⁻⁴ m². The maximum ΔT for the ribbon segment is about 500 K which results in 0.2 mW of power dissipation through conduction. Therefore, the power transferred through conduction is insignificant when compared to the overall power and can be neglected.

The power out due to convection and radiation is given by,

$$P_{conv} + P_{rad} = [h(T_s - T_\infty) + \epsilon \sigma T_s^4] A$$

where h is the average heat conduction coefficient, T_s is the surface temperature of the ribbon, T_∞ is the temperature of the atmosphere, ϵ is the emissivity of the ribbon material, and σ is the Stephan-Boltzmann constant. The emissivity of most non metal materials is approximately 0.9 (Carroll, J.A., 1985), σ is a constant equal to 5.67 x 10⁻⁸ W/m²-K⁴, and the background temperature at 25 km is approximately -56 °C. Therefore, in the heat transfer equation above, the average heat conduction coefficient is the only unknown variable.

The average heat conduction coefficient depends on the Reynolds number which indicates if the flow is laminar or turbulent. The accepted value of the Reynolds number at

Fisher Space Systems, LLC

which transition occurs is 5×10^5 . A Reynolds number below this value indicates laminar flow while a number above this value indicates turbulent flow. The Reynolds number is given by,

$$R_e = \frac{(\rho v x)}{\mu}$$

where ρ is the density of the atmosphere equal to $4.1 \times 10^{-2} \text{ kg/m}^3$, v is the velocity of the ribbon segment equal to 315 m/s, x is the width of the ribbon equal to 1.0 m, and μ is the viscosity equal to $1.425 \times 10^{-5} \text{ kg/m-s}$ (Fox, R.W. and McDonald, A.T., 1992). From the above equation, the Reynolds number is about 9×10^5 . This indicates that the flow may be turbulent at the trailing edge with the transition occurring at about 70 cm. Since the flow is laminar for the most part of the ribbon, calculating the average heat conduction coefficient will be based on laminar flow.

Assuming laminar flow, the average heat conduction coefficient is given by,

$$h_{avg} = 0.664 R_e^{1/2} Pr^{1/3} \frac{k_f}{x}$$

where Pr is the Prandtl number equal to 0.731 and k_f is the thermal conductivity of the air at 217 K equal to $1.954 \times 10^{-2} \text{ (W/m-K)}$ (Incropera, F.F. and DeWitt, D.P., 1985). From the above equation, the average heat conduction coefficient is approximately $11 \text{ W/m}^2\text{-K}$. Inserting the the known variables into the heat transfer equation above, doing the math, and combining like terms gives,

$$868 \text{ K} = T_s + (5 \times 10^{-9} / \text{K}^3) T_s^4$$

Solving for the surface temperature requires an iteration procedure starting at a best guess surface temperature for the ribbon. The maximum recommended temperature range for long term use in air for Kevlar 49 is from 422 K to 450 K (Kevlar, 2012). Starting at 450 K and increasing in incremental steps gives the surface temperature for the 10 m segment of ribbon at about 515 K. This is slightly higher than the recommended maximum operating temperature but, it is good enough for a preliminary result.

The power required to rotate two ribbons is given by the aerodynamic drag equation above. By adding the power resulting from each 10 m segment of ribbon, the total power required to overcome drag and rotate the ribbon is about 4 MW. To restore the kinetic energy of rotation after launch requires an additional megawatt of power bringing the total for one ribbon up to 5 MW. Therefore, with two ribbons, the power required is approximately 10 MW.

In summary, power into the ribbon due to aerodynamic drag, solar radiation, and Earth's albedo limits the ribbons length to approximately 2 km. The last 10 m segment of the ribbon experiences the highest temperature. Heat transfer occurs primarily by convection and

Fisher Space Systems, LLC

radiation resulting in a surface temperature of approximately 515 K. Finally, high temperature superconducting motors producing around 8 - 10 MW of power are required to rotate the two ribbons.

2.a.2. Counterweight

The kinetic energy of rotation (KER) must be several orders of magnitude greater than the kinetic energy of launch. This is to keep the ribbon from dropping into a higher density atmosphere which may result in a higher surface temperature of the ribbon. To meet this requirement for a 2 km ribbon, the mass of the counterweight should be about 25 ton. From the Flexible Ribbon Model (Fisher, J.F., 2012), the mass of the ribbon and counterweight together is approximately 29 ton.

Also, from the Flexible Ribbon Model, the moment of inertia of the ribbon and counterweight is on the order of 10^{11} kg-m² resulting in a KER on the order of 10^9 J. The kinetic energy of launch is 10^7 J. The change in kinetic energy results in a 3% decrease in angular velocity and drops the ribbon angle from 79° to 78°. The last 10 m segment of ribbon therefore, drops into a slightly higher density atmosphere and the surface temperature increases slightly. The decomposition of Kevlar in air is from 700-755 K (Kevlar, 2012). So, a slight increase in temperature can be tolerated for a brief period. However, to compensate for the slight increase, the angle of attack of the ribbon can be reduced by designing the counterweight as a fuselage with a tail boom and elevator. Reducing the angle of attack reduces drag and keeps the surface temperature below the maximum safe operating limit until the electric motors restore KER to the ribbon. With 2 MW of power available from the electric motors, the KER is restored in less than a minute.

In addition to adjusting the ribbon's angle of attack, the counterweight must be designed to withstand the high g loading resulting from rotation, absorb the shock due to launch, and dampen the vibrations of the ribbon. Therefore, the counterweight contains within its structure the necessary batteries, flywheels, motor generators, spindles, gears, electronics, and extra ribbon required to perform the task. A preliminary design is shown in figure 2 below.

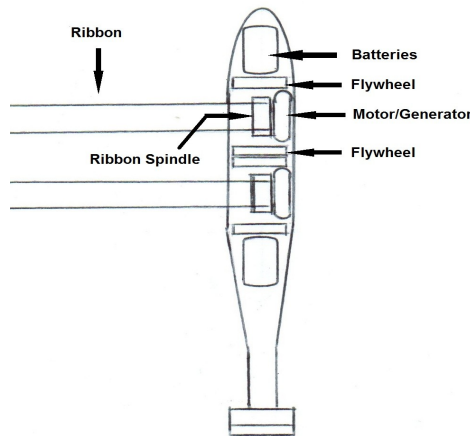


Figure 2. Counterweight

Fisher Space Systems, LLC

2.b. Launch Vehicle and Overcarriage

The launch vehicle for the proof of concept system is a suborbital second stage. The maximum altitude is approximately 100 km. Since the launch vehicle travels down the ribbon and the angle of the ribbon is about 79° from the vertical, it will have a small velocity directed downward. The launch vehicle needs to recover from this downward velocity. The slight increase in ΔV increases the mass of the second stage. As detailed below, the estimated mass of the suborbital launch vehicle (SLV) is 2450 kg.

The overcarriage (OC) has several functions. First, the OC carries the second stage launch vehicle to the launch point. Also, the OC remains on the ribbon after launch. As it travels down the ribbon and continues to accelerate, the Coriolis force increases on the OC. The increase in force results in a dampening affect on the ribbon. Therefore, the shock wave produced by the launch is greatly reduced. When the spring back velocity of the ribbon approaches zero, the OC separates from the ribbon via an on board propulsion system, deploys a ram air para-foil, and returns to the launch site. As detailed below, the estimated mass of the OC is about 830 kg. Together, the SLV and OC have a combined mass of 3280 kg.

2.b.1 Suborbital Launch Vehicle

The mass estimate for the suborbital launch vehicle (SLV) is derived using the mass estimating relationships compiled by Georgia Tech (Rohrschneider, R.R., 2002). The Georgia Tech database uses a number of different relationships to estimate the mass of individual components for the flight vehicle. Georgia Tech uses the Space Shuttle for its relationship comparison. It is recommended that the user select the relationship that results in the closest comparison to a known flight component. The main fuselage with crew cabin of the SLV is more closely related to a Mercury space capsule than to the Space Shuttle in design. Therefore, the relationships resulting in the correct weight for the Mercury space capsule will be used for the SLV.

Individual components for the Mercury space capsule were selected from the George Tech database, the weights were determined, added together, and compared to the end of reentry weight for the Mercury space capsule No. 20 (Project Mercury, 1963). The results are shown in table I below. The weight using the Georgia Tech database shows approximately a 2% difference from the end of reentry weight of the Mercury space capsule. These relationships, as identified by the reference numbers, will be used for the individual components of the SLV.

Fisher Space Systems, LLC

Component	Reference	Weight Estimate (lb)
Body (Fuselage & Cabin)	6	612
Thermal Protection	6	247
Reaction Control	3	37
Prime Power	1	249
Elec. Conver. & Dist.	3	164
Surface Control Actuators	3	13
Avionics	4b & 7	615
Environ. Cont. & Life Support	1	437
Personal Equipment	4b	52
Crew & Gear	4b	256
Total	Dry Weight	2682
No. 20 End of Reentry	Qtr Status Rpt.	2637
% Difference		2%

Table I. Mercury No. 20 Estimated Weight

The main fuselage with crew cabin of the SLV will be designed similar to the Mercury space capsule. The main difference in design is the method of launch (i.e. hanging down from an overcarriage instead of on top of a booster), the addition of the ram air parafoil, the propellant tanks, the H₂O₂/RP-1 rocket engine and nozzle, and the duration of flight and the recovery method. To demonstrate proof of concept, the suborbital launch vehicle will separate from the overcarriage and the rotating ribbon at an altitude of approximately 25 km, boost under thrust, coast to a peak altitude greater than 100 km, reenter, and land on a runway using a ram air parafoil. The mass estimates are shown in table II and a conceptual design is shown in figure 3 below.

Fisher Space Systems, LLC

Component	Reference	Weight Estimate (lb)
Body (Fuselage & Cabin)	6	977
Thermal Protection	6	245
Landing Gear	6	58
Main Propulsion	3	187
Reaction Control	3	42
Prime Power	1	154
Elec. Conver. & Dist.	3	139
Surface Control Actuators	3	14
Avionics	4b & 7	352
Environ. Cont. & Life Support	1	289
Personal Equipment	4b	52
Total (Sum of 1st 11 rows)	Dry Weight	2509
Dry Weight Margin	10%	251
Crew & Gear	4b	256
Residual Prop.	1	22
RCS Entry Prop.	1, 2, & 10	17
RCS On-Orbit Prop.	1	63
Inflight Losses	2, 3, & 10	30
Start Up Losses	1	5
Ascent Propellant	1, 2, & 10	2248
GLOW (GLOM)		5401 (2450 kg)

Note: Weights include the technology reduction factors as recommended by the Georgia Tech study.

Table II. Suborbital Launch Vehicle Estimated Weight

Fisher Space Systems, LLC

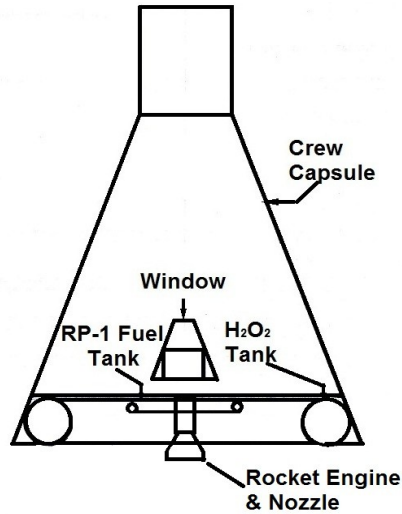


Figure 3. Suborbital Launch Vehicle

2.b.2. Overcarriage

The overcarriage (OC) is an integral part of the Space Track Launch System. Without the OC, the potential energy stored in the ribbon would release in the form of a shock wave. The shock wave would travel up the ribbon and strike the tower. This could possibly destroy the ribbon and the tower. As a minimum, the top of the tower and the ribbon would have to be replaced after every launch. Analysis shows that the OC arrests the spring back of the ribbon and helps to eliminate the shock wave.

As with the SLV, the mass of the OC is determined using the mass estimating relationships compiled by George Tech (Rohrschneider, R. R., 2002). From the data compiled by George Tech, the mass is determined to be approximately 830 kg and when added to the mass of the SLV gives a total mass of 3280 kg.

2.b.3. Ribbon Displacement and Recoil

The displacement of the ribbon from its normal position is shown in figure 4 below. The displacement is due to the Coriolis force on the launch vehicle and overcarriage as it travels down the ribbon to the launch point. This is very similar to the dynamic stability of the ribbon for the space elevator (de Vries, J., 2006).

Fisher Space Systems, LLC

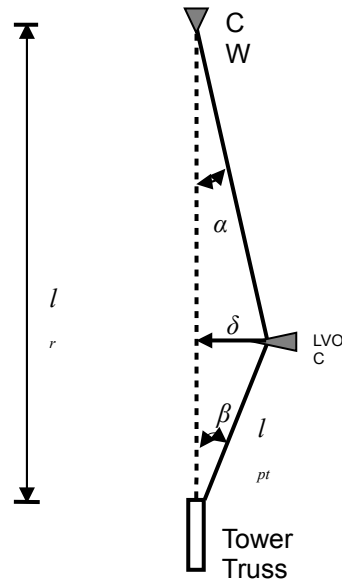


Figure 4. Displacement of Ribbon due to Launch

From the Delft University of Technology final report, the displacement due to the Coriolis force is given by,

$$\delta_{max} = l_{pt} \left(1 - \frac{l_{pt}}{l_r}\right) \left[\frac{(2 \omega v_r m_{LVO C})}{T_{pt}}\right]$$

where δ_{max} is the maximum displacement of the ribbon just prior to launch, l_{pt} is the launch point along the ribbon, l_r is the ribbon length, ω is the angular velocity of the ribbon, v_r is the radial velocity at launch, $m_{LVO C}$ is the mass of the launch vehicle and overcarriage, T_{pt} is the tension in the ribbon at the launch point, α is the displacement angle at the counterweight, and β is the displacement angle at the tower truss.

For the proof of concept system and with a CW mass equal to 25 tons, the tension in the ribbon at the launch point, T_{pt} , is approximately 1.4×10^6 N (Fisher, J.F. , 2012), the angular velocity, ω , is 0.16 rad/s, the radial velocity, v_r , is about 162 m/s, and the launch point, l_{pt} , is around 1 km. This results in a displacement, δ_{max} , of the ribbon from its normal position at launch of 60 m. Since the launch point is half the distance of the ribbon length, the displacement angles, α & β , are both equal at 3.4° . These parameters are used to set up the analysis at launch of the second stage.

At launch, the mass on the ribbon drops from 3280 kg to 830 kg (the mass of the OC). As such, the Coriolis force still acting on the overcarriage is greatly reduced to 4.3×10^4 N. The force acting in the opposite direction due to the tension in the ribbon is given by,

Fisher Space Systems, LLC

$$F_t = F_\alpha + F_\beta = 1.4 \times 10^6 * \sin(\alpha) + 1.4 \times 10^6 * \sin(\beta) = 1.7 \times 10^5 \text{ N}$$

The sum of the forces, $1.3 \times 10^5 \text{ N}$, is equal to the mass of the OC times its acceleration (Newton's 2nd Law). Allowing this acceleration to act on the OC over a 1 m distance results in a velocity of the ribbon back toward its normal position given by,

$$v_f^2 = v_i^2 + 2as$$

where v_f is to be determined, v_i is the initial velocity of the ribbon equal to 0 m/s at $t = 0 \text{ sec}$, a is the acceleration equal to 152.4 m/s^2 , and s is the increment equal to 1 m. This results in a velocity of 17.5 m/s in the direction toward its normal position. The average time it takes for the OC and ribbon to move a distance of 1 m is approximately 0.1 seconds. The OC travels a distance of 18.5 m during this time. Its radial velocity increases slightly and the Coriolis force acting on the OC increases slightly. New displacement angles are calculated and the process is repeated. A spreadsheet was developed to handle the calculations. The results (at 10 m increments) are shown in table III below.

Displacement (m)	Sum of the Forces (N)	Ribbon Acc (m/s ²)	Ribbon Velocity (m/s)
60	1.3×10^5	152	18
50	9.8×10^4	117	55
40	6.9×10^4	83	70
30	4.0×10^4	48	79
20	1.0×10^4	13	82
10	-1.9×10^4	-23	81
0	-4.9×10^4	-59	76
-10	-7.9×10^4	-96	65
-20	-1.1×10^5	-134	43
-27	-1.4×10^5	-164	0

Table III. Ribbon Velocity after Launch

The velocity of the ribbon increases to a peak of 83 m/s before the Coriolis force acting on the OC becomes greater than the total force resulting from the tension in the ribbon. The ribbon begins to slow down, it passes through its normal position, and comes to rest with a displacement of approximately 27 m on the other side of normal. At this point, the OC launches off the ribbon. The remaining oscillations are dampened by the CW. The retarding force of the overcarriage and the energy absorbed by the counterweight act together to reduce the shock in the ribbon at launch.

Fisher Space Systems, LLC

2.c. Truss, Gear Assembly, Motors, and Transfer Station

The rotating truss attaches to the ribbon and serves as a lever arm for the ribbon. Its mass depends on the counterweight mass, the ribbon mass, and the launch vehicle and overcarriage mass. The gear assembly consists of a turntable, power divider ring, reduction gears, and main drive gears. There are four 2.5 MW high temperature superconducting electric motors that drive the power divider ring. At the transfer station, the second stage launch vehicle and the OC transfer from the climber to the lift. The lift raises the SLV and OC to the rotating truss. The estimated mass of the truss, gear assembly, motors, and transfer station is 289 metric tons.

2.c.1 Rotating Truss

The design of the rotating truss is based on a box beam design and is constructed using a new high strength composite called M5[®] (M5[®], 2006). The M5[®] material has a density of 1700 kg/m³, an ultimate compression strength of 2 GPa, a working compression strength of 667 MPa (a safety factor of 3), and a Young's modulus of 330 GPa. For the proof of concept tower, the ribbon length is 2 km and the counterweight (CW) reels itself in and lets itself out during the stop and start phases of rotation. Therefore, a cradle is required to support the CW during down times and maintenance.

After the CW reels itself in and the truss stops rotating, the CW lowers itself onto the cradle and is secured. Counterweight inspection, maintenance, assembly and dis-assembly (CIMAD) robots break the CW into sections, remove the flywheels and batteries, disconnect the ribbon, and transport the disassembled parts to ground stations for inspection, repair, and maintenance. Modifications and upgrades to the CW are performed at this time. The CW is then returned to the truss, reassembled by the CIMAD robots, the ribbons are reattached, rotation started, and the CW reels itself back out to 2 km. A cross section of the tower is shown in figure 5 below. The mass of the rotating truss and cradle is an estimated 46 metric tons.

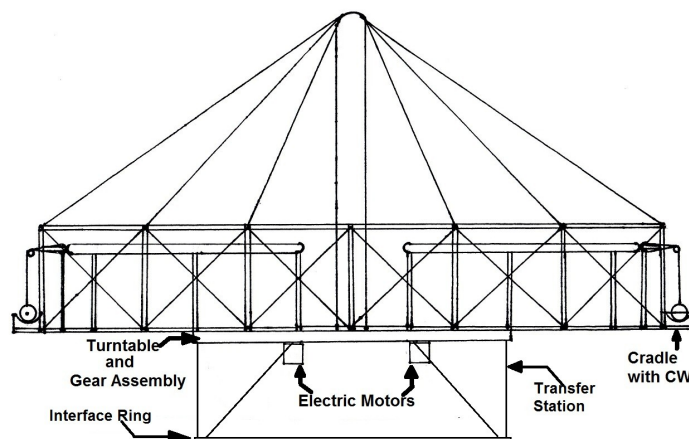


Figure 5. Rotating Truss

Fisher Space Systems, LLC

2.c.2 Turntable and Gear Assembly

The turntable consists of an upper rotating table and a lower support table. The upper rotating table supports the rotating truss and tension towers. The table is held into position by the gear assembly. There are 20 identical gear sets that make up the gear assembly. The total load on the upper rotating table is 1.1×10^6 N. To accommodate the truss and the tension towers, the upper table has an inner diameter of 30 m and an outer diameter of 33 m. The estimated mass of the upper and lower table is 25 metric tons.

The upper rotating table is held into position by the gear assembly. The gear assembly is shown in figure 6 below. There are 20 identical gear sets that make up the gear assembly. The gear assembly is driven by a power divider ring. The power divider ring is required to shift from the shaft speed produced by the electric motors down to the rotation rate of the turntable (approximately 1.5 rpm). If not for the power divider ring, the face width of the gears would be too wide resulting in massive gears. The estimated mass of the gear assembly is 29 metric tons. The total mass of the upper turntable, lower turntable support, and the gear assembly is approximately 54 metric tons.

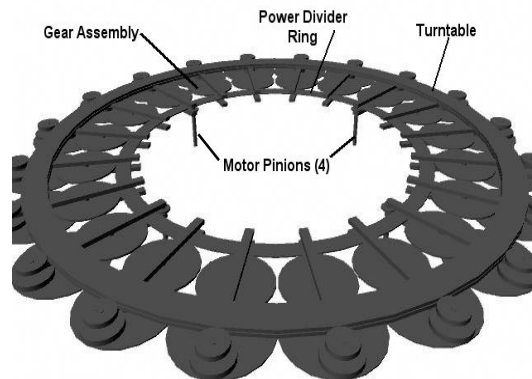


Figure 6. Turntable and Gear Assembly

2.c.3. High Temperature Superconducting Electric Motors

The turntable, gear assembly, and power divider ring are driven by four 3,350 hp high temperature superconducting motors (American Superconductor, 2010). Each motor has an estimated mass of 12.5 metric tons and produces its maximum torque at 230 rpm. The power transferred from the HTS motors to the power divider ring is approximately 13,400 hp. The mass of four HTS motors is approximately 50 metric tons.

2.c.4. Transfer Station

The turntable and gears are supported by 20 braces attached to a load bearing ring.

Fisher Space Systems, LLC

The ring serves as the interface between the rotating structure and the torque buffer (figure 7). Each brace is made up of a column, a horizontal gear support, and a strut. Since the column supports the maximum load, the mass estimate for the brace will be based on load requirements of the column.

Each column supports a load of 6.7×10^4 N. The braces provide the structure for the transfer station. There is an outer ring and an inner ring at the base of the gears to handle the lateral stresses. Both rings are of the same area dimension as the brace. The mass of 20 braces, the inner ring, and the outer ring is an estimated 16 metric tons.

The inner surface of the transfer station is modeled as a truncated cone with a base radius of 16 m, a height of 6 m, and a top radius of 11 m. The outer surface of the transfer station is modeled as a cylinder with a radius of 17 m and a height of 6 m. The station is hollow through the center to allow transfer of the 2nd stage SLV to the rotating truss. The station is bounded on the top by the gear assembly and on the bottom by the interface ring. The station has an estimated mass of approximately 59 metric tons.

The rotating truss and the transfer station are connected to the torque buffers by an interface ring. The interface ring has a radius of 16.5 m and supports a load of approximately 2.6×10^6 N. There are 100 support towers each 1.0 m in diameter. Therefore, each tower supports 2.6×10^4 N and the distance between the supports should a tower fail or needs to be replaced is about 2.0 m. This results in a thickness of 17 cm and an estimated mass of 29 metric tons.

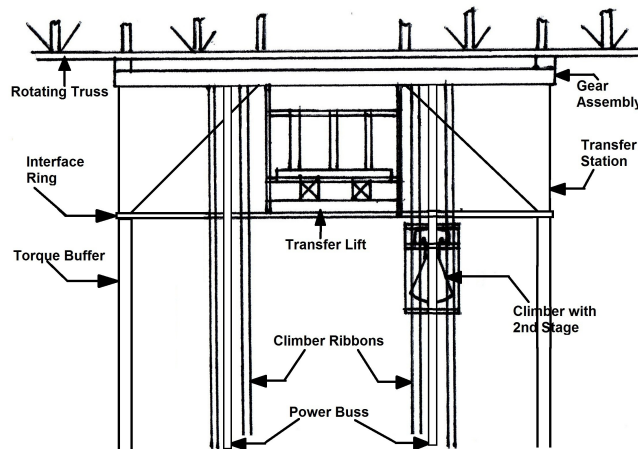


Figure 7. Transfer Station

2.c.5. Transfer Lift and Climbers

The overcarriage and second stage launch vehicle, when fueled, have a mass of 3280 kg. The lift table consists of the second stage support structure which rests on a rotating table and is lifted into position by two scissor jacks. The jacks rest on a support base which in turn rests on support trusses which are mounted to the transfer station. The estimated mass of the

Fisher Space Systems, LLC

transfer lift is 6,050 kg.

The climbers transport the SLV and OC from the base station to the transfer lift. There are two climbers. Each climber has a support structure, base, frame, and climber motor assembly. The total mass is approximately 6,400 kg each. With two climbers, the mass is 12.8 tons.

2.c.5.a Transfer Lift

The lift transfers the SLV and the OC to the rotating truss. The lift has tracks to support the SLV and OC, braces to support the tracks, and a base to support the braces. There are two tracks each 8 m long, a half meter wide, and 10 cm thick. Each track is attached to three braces. Each brace consist of a 2.5 m beam, a 5.6 m strut, and a 5 m column. The mass of the six braces and two tracks is approximately 1,700 kg.

The second stage support structure is lifted into position by two scissor jacks. Scissor jacks with lifting capacities over 5 metric tons are commercially available (ECOIA Industrial Products, Inc., 2004). Each jack has a shipping mass of approximately 1,000 kg.

The scissor jacks rest on a platform base. The platform has a thickness of approximately 2.5 cm. With a surface area of 64 m², the platform base has a mass of approximately 2,700 kg. All together the mass of the tracks, braces, scissor jacks, and platform base is approximately 6,050 kg.

2.c.5.b Climbers, Ribbons, and Power Buss

The climbers transport the SLV and OC from the base station to the transfer lift. There are two climbers. Each climber has a support structure, base, frame, and climber motor assembly. The total mass is approximately 6,400 kg each. With two climbers, the mass is 12.8 tons.

When transporting the SLV and OC, the mass of the climber is about 9,680 kg. Each climber climbs up four Kevlar ribbons attached to a support frame on the transfer station. The four ribbons have a mass of 5,200 kg. The mass required to support two climbers is about 10.4 tons.

The electrical power for the climbers and rotating truss is transmitted to the station by Kevlar ribbons with a thin conductor coating such as aluminum. High voltage power lines made of aluminum typically have a cross section of approximately 12 mm². For a 25 km long transmission line, the mass of aluminum is approximately 810 kg. The half meter wide Kevlar ribbon is coated with the aluminum conductor bringing the total mass of one transmission line to about 1,240 kg. Each climber has two conductors, a positive and a negative, bringing the total mass to 2,480 kg. With two climbers, the mass is about 5 ton.

The total mass hanging from the support structure at the transfer station is about 28 ton. Along with the transfer lift, brings the total load supported by the structure to 34 metric

Fisher Space Systems, LLC

tons. The support structure is of a box beam design similar to the rotating truss. Its mass is about 46 metric tons.

In summary, the total static load on the torque buffer is an estimated 3.8×10^6 N and is summarized in table IV below. During torque buffering and pressure stabilizing, there is an additional load of 2.1×10^6 N. Therefore, the peak dynamic load at the top of the torque buffer is an estimated 5.9×10^6 N.

Component	Estimated Mass
Ribbon & CW (x2)	58,000 kg
SLV & OC (x2)	6,560 kg
Rotating Truss	46,000 kg
Turntable	25,000 kg
Gear Assembly	29,000 kg
Motors	50,000 kg
Transfer Station	59,000 kg
Interface Ring	29,000 kg
Transfer Lift	6,050 kg
Climbers	12,800 kg
Climber Ribbons	10,400 kg
Power Buss	5,000 kg
Support Structure	46,000 kg
Total Mass	382,810 kg
Load	3.8×10^6 N

Table IV. Tower Static Load

3.0 Inflatable Beam Tower

For the proof of concept system, the tower is approximately 25 km high. The tower is made of Kevlar beams. The first 100 m of the support tower is called the torque buffer. The torque buffer removes the torque produced by the electric motors. Also, the torque buffer is used to assist in stabilizing the tower. The tower experiences an unbalanced force due to the rotation of the ribbons and counterweights. From ground level, the first 13 km of inflated beams is filled with air and the next 12 km is filled with hydrogen. The air filled beams have air cells every 100 m while the hydrogen filled beams have cells every 500 m.

Fisher Space Systems, LLC

3.a Torque and Precession

Torque is produced when the electric motors restore rotational kinetic energy to the system and precession occurs due to an unbalanced lateral load at the top. Both torque and precession are controlled by a 100 m section of inflated beams called a torque buffer. The torque buffer bleeds off the torque produced by the electric motors during restoration of rotational kinetic energy. Precession is due to an unbalanced lateral force at the top of the tower. Gyroscopic stabilization helps to prevent tip displacement due to the unbalanced force. Pressure variation in the inflated beams is used to keep the lateral force from setting up uncontrollable oscillations and keep tip displacement to a minimum.

3.a.1 Torque

A torque of approximately 6.25×10^7 N-m is produced at the top of the tower when rotational kinetic energy is restored after launch. If not removed, the torque would exceed the critical bending moment of the beams. The torque is removed by a 100 m section of tower called the torque buffer.

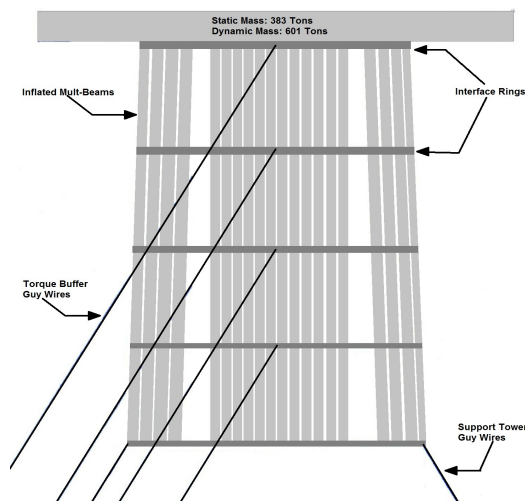


Figure 8. Torque Buffer

As shown in figure 8, the torque buffer is made up of 4 layers. Each layer has approximately 100, 25 m long 1 m diameter ($L/D = 25$, Euler beam theory applies) inflated beams pressurized with hydrogen. Each layer is separated by an interface ring connected to four guy wires which are connected tangentially to the ring at a 30° angle to the axis. The guy wires produce an opposing force of about 2.4×10^5 N per wire. Each layer removes about 1.6×10^7 N-m of torque from the system. At a radius of 16.5 m, the lateral force on each beam is 9.5×10^3 N. The beams are 25 m long, therefore, the moment is approximately 2.4×10^5 N-m.

For an inflated beam, the moment is given by (R.K. Seth, B.M. Quine, and Z.H. Zhu, 2009),

Fisher Space Systems, LLC

$$\text{Beam Moment} = 0.4\pi\sigma_w tR^2$$

where σ_w is the working tensile strength for Kevlar equal to 1.2×10^9 N/m², t is the thickness of the beam fabric equal to 1.0 mm, and R is the radius of the beam equal to 0.5 m. Inserting the variables gives the beam moment equal to 3.8×10^5 N-m. The beam moment is greater than the peak beam moment produced during torque buffering.

The estimated load at the first layer is 3.8×10^6 N. The interface ring at the base of the transfer station has four guy wires. While torque buffering, the guy wires produce a peak additional load of 2.1×10^6 N. As such, the peak load on the first layer of beams is an estimated 5.9×10^6 N. The maximum payload capacity of each inflated beam is given by (R.K. Seth, B.M. Quine, and Z.H. Zhu, 2009),

$$MPC = \frac{\sigma_u}{\left(\frac{R}{t}\right)} - \frac{(2H\rho g)}{\left(\frac{R}{t}\right)} - H\rho'_g g$$

where σ_u is the ultimate tensile strength of Kevlar equal to 3.6×10^9 N/m², R is the radius of the beam, t is the thickness, H is the length equal to 25 m, ρ is the density of Kevlar equal to 1440 kg/m³, g is equal to 9.81 m/s². and ρ'_g is given by,

$$\rho'_g = \frac{\mu\sigma_u}{R_g T \left(\frac{R}{t}\right)}$$

where μ is the molecular weight of hydrogen equal to 2×10^{-3} kg/mol, R_g is the gas constant equal to 8.314 J/K-mol, and T is the temperature at 25 km equal to 217 K. Inserting the variables gives the maximum payload capacity for each beam equal to 3.6×10^6 N/m². The area for each beam is about 0.8 m² and there are 100 beams. Therefore, the maximum load is 2.8×10^8 N. The maximum load capacity is well above the peak dynamic load of 5.9×10^6 N.

The critical buckling load for the all 100 beams is given by (Seth, 2010),

$$P_{cr} = \frac{\pi^2 E' I}{L_e^2}$$

where E' is the effective modulus of Kevlar equal to 131×10^9 N/m² and L_e is the length of the inflated beam equal to 25 m. It is important to note that the effective modulus is equal to the material modulus at a certain minimum pressure and increases with an increase in pressure (Seth, 2010). More research is required to establish this relationship. At present, the E' will be set equal to the material modulus.

Fisher Space Systems, LLC

The area moment of inertia, I , is given by (R.K. Seth, B.M. Quine, and Z.H. Zhu, 2009),

$$I = N(\pi R t (R^2 + r^2))$$

where N is the number of inflated beams equal to 100 and r is the radius of the torque buffer equal to 16.5 m. Inserting the variables gives the area moment of inertia equal to 42.8 m⁴ and the critical load equal to 8.8 x 10¹⁰ N. The critical load capacity is about 4 orders of magnitude above the peak dynamic load.

Each beam has a mass of approximately 113 kg with a gas mass of about 78 kg. In total, the 100 beams add an additional load of 1.9 x 10⁵ N. Adding the mass of the 400 beams, the hydrogen gas, 16 guy wires, and 4 interface rings gives a total dynamic load on the support towers of approximately 1.5 x 10⁷ N.

3.a.2. Precession

The tower will want to precess due to an unbalanced lateral load at the top. This lateral load is caused by the difference in force due to the rotation of the Earth and its effect on the center of mass of the ribbons and counterweights. The maximum force occurs at the equator when the velocity of the center of mass is in the same/opposite direction as the tangential velocity of a point on the Earth. For example, when looking down on the tower and the tower is rotating in a counterclockwise direction, the tangential velocity of the center of mass on the southern side is approximately +463 m/s and the tangential velocity of the center of mass on the northern side is approximately -463 m/s. This results in a maximum lateral force of 2.2 x 10⁶ N in the southern direction.

The precession is held in check by two methods, gyroscopic stabilization and pressure variation in the inflated beams. First, there is a gyroscopic stabilization of the tower. The Space Track Launch System is basically a large gyroscope. Tip displacement will be opposed by a restoring force setup by the angular momentum of the tower. The restoring force is given by,

$$F_x = \frac{L_z}{h_g^2} \left(\frac{dS}{dt} \right) \quad (\text{Seth, 2010})$$

where L_z is the angular momentum of the tower, h_g is the height above ground and dS/dt is the tip displacement velocity. In accordance with theory, the faster the displacement, the stronger the restoring force.

Second, the lateral force will eventually set up a displacement and the oscillation will grow out of control. Therefore, the pressure in the beams on the leeward side will increase to offset this displacement. Using a combination of gyroscopic stabilization and pressure variation in the beams, the tip displacement can be kept at a minimum.

In summary, each of the four layers of inflated beams removes 1.6 x 10⁷ N-m of torque

Fisher Space Systems, LLC

and each inflated beam in each layer experiences a bending moment of 2.4×10^5 N-m. As presently designed each beam can withstand a critical bending moment of 3.8×10^5 N-m. Precession is kept in check by gyroscopic and pressure stabilization. Finally, the dynamic peak load on the support tower is 1.5×10^7 N.

3.b Support Tower

As mentioned in section 3.a above, the dynamic peak load on the support tower is approximately 1.5×10^7 N. At this point, the torque buffer has removed all lateral forces on the towers making the critical buckling load the driving design parameter. The support tower analysis is based on a dissertation written by Raj Kumar Seth (Seth, 2010).

The beams at altitudes of 13 km and above are filled with hydrogen and the beams below 13 km are filled with air. All beams except the beams at ground level have a length, L , equal to 1.5 km, a radius, R , equal to 1.0 m, and a thickness, t , equal to 0.75 mm. This results in a material mass of each beam of approximately 10 tons. This material mass permits the difficult but doable task of maintenance, repair, and replacement. Maintenance, repair, and replacement is done by beam inspection, maintenance, and equipment repair robots (BIMERRs). The BIMERRs will be designed to remove and replace a beam in the event that the beam cannot be repaired on site. The beams at ground level can be greater in length because removal and replacement is done at ground level.

At a fixed beam length of 1.5 km, the critical buckling load depends on two variables, the area moment of inertia, I , and the effective modulus of elasticity, E' . With a fixed beam radius of 1.0 m and a thickness of 0.75 mm, the area moment of inertia is dependent on two more variables, the number of beams, N , and the radius, r , of the multi-beam structure. The support tower beams can only be tilted at an angle of 0.1° before exceeding the beam moment.

By bracing the beams at selected intervals, the beams can be tilted at a greater angle resulting in a more stable platform. For example, if the beams are braced at 500 m intervals, the tilt angle can be increased to 1° . If the beams are braced at 100 m intervals, the tilt angle can be increased to 5° . It may be possible to eliminate the guy wires and have a free standing tower. However, bracing the towers at selected intervals and increasing the tilt angle results in heavier loads and more beams. The advantages and disadvantages must be considered.

At present, to meet the critical buckling load requirement at ground level, it is important to start at a large radius of 20 m at the top. The torque buffer cylinders are only 25 m in length and can be tilted at greater angles. Therefore, it is possible to increase the radius of the torque buffer from 16.5 m at the top to 20.0 m at its base without exceeding the beam moment of the torque buffer beams.

The critical buckling load also depends on the effective modulus of elasticity, E' , of the beam. At a certain pressure, the effective modulus of elasticity of an inflated beam is equal to the modulus of elasticity of the material. For the present analysis, E' is set equal to 131 GPa, the modulus of elasticity of Kevlar 49. However, according to theory, the effective modulus of

Fisher Space Systems, LLC

elasticity depends on the internal gas pressure of the inflated beam (Seth, 2010). As the gas pressure increases above a certain pressure, the modulus of elasticity of the beam increases. With reference to the critical buckling load equation, the advantage of this increase is obvious. Fewer beams will be required to support a given load or heavier loads will be possible with a given number of beams.

Beginning at the base of the torque buffer, it takes 24 beams to support a peak dynamic load of 1.5×10^7 N. The 24 beams are supported by an interface ring with guy wires attached for stability. To reduce mass, the beams are divided into four clusters connected with a support ring. For the hydrogen filled beams, the clusters are arranged in a 2 beam deep fashion. For example, at the first interface ring at 25 km, the clusters are arranged in a 2 beam by 3 beam matrix. For the second interface ring at 23.5 km, the clusters are arranged in a 2 beam by 4 beam matrix. The cluster arrangement is illustrated in figure 9 below. Keeping the clusters 2 beams deep not only reduces mass of the interface ring but also simplifies maintenance, repair, and replacement of the beams.

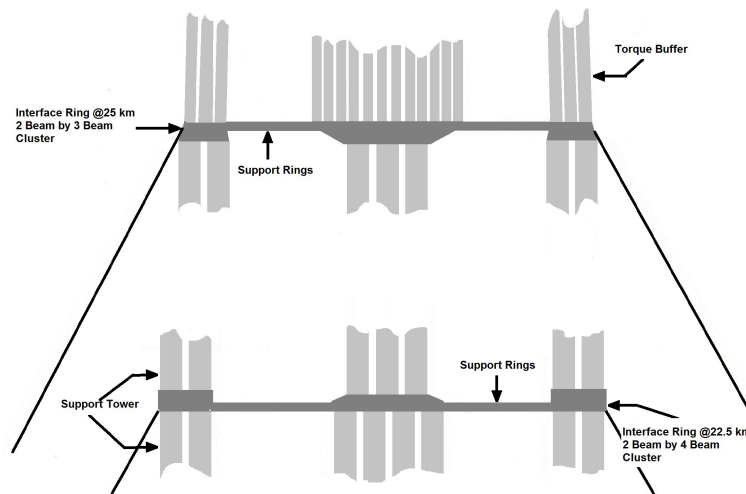


Figure 9. Beam Cluster Arrangement

Because of the slight angle, the radius of the interface ring increases resulting in a corresponding increase in the area moment of inertia for the multi-beams and the critical buckling load. A spreadsheet was developed to handle the calculations inserting the appropriate values for the hydrogen gas density at various altitudes and then switching to air below 13 km. The results are shown in table V below.

Fisher Space Systems, LLC

Altitude (km)	Load (N)	# of Cyl.	Pcr (N)	MPC (N)
$25 \leq H \leq 23.5$	1.5×10^7	24	1.5×10^7	2.0×10^8
$23.5 \leq H \leq 22$	2.2×10^7	32	2.5×10^7	2.6×10^8
$22 \leq H \leq 20.5$	3.1×10^7	40	3.8×10^7	3.3×10^8
$20.5 \leq H \leq 19$	4.3×10^7	40	4.6×10^7	3.3×10^8
$19 \leq H \leq 17.5$	5.5×10^7	48	6.6×10^7	3.9×10^8
$17.5 \leq H \leq 16$	7.0×10^7	48	7.7×10^7	3.9×10^8
$16 \leq H \leq 14.5$	8.4×10^7	48	8.9×10^7	3.9×10^8
$14.5 \leq H \leq 13$	9.9×10^7	48	1.0×10^8	3.9×10^8

Table V. Support Tower, Hydrogen Fill

At 13 km, the fill gas is switched to air. Helium would make a better fill gas. But, at present, it is uncertain as to the cost advantage. Air is a larger molecule and therefore, will not dissipate through the material as rapidly as helium and is, of course, cheaper. Also, if theory holds, increasing the pressure will increase the effective modulus of elasticity, E' , of the inflated beams. As such, fewer beams will be required to meet the load demands.

The four clusters that make up the interface ring are switched to a three beam deep arrangement. It is a little more difficult to maintain, repair, or replace the beams but still possible. The three beam deep arrangement is necessary to fit all of the beams required to support the load into the available space.

At altitudes less than 11 km, the temperature is no longer a constant -56°C but varies according to altitude. This has a slight negative impact on the maximum payload capacity. As a result, the number of cylinders required to support the load rapidly increases to 600 at 2.5 km.

At an altitude of 2.5 km, the length of each beam can be increased to 2.5 km and its thickness to 2.5 mm. This results in a mass of about 57 tons per beam. To replace the beams, BIMERRs will guide the beam as it is deflated. A heavy lift crane will remove the beam and replaced it with a new beam. The BIMERRs will then guide the new beam as it is inflated. The spreadsheet continues with new variables pertaining to air and the change in temperature. The results are shown in table VI below.

Fisher Space Systems, LLC

Altitude (km)	Load (N)	# of Cyl.	Pcr (N)	MPC (N)
$13 \leq H \leq 11.5$	1.1×10^8	56	1.4×10^8	3.6×10^8
$11.5 \leq H \leq 10$	2.4×10^8	96	2.6×10^8	6.2×10^8
$10 \leq H \leq 8.5$	4.4×10^8	144	4.4×10^8	9.4×10^8
$8.5 \leq H \leq 7$	7.2×10^8	216	7.4×10^8	1.4×10^9
$7 \leq H \leq 5.5$	1.1×10^9	300	1.1×10^9	2.0×10^9
$5.5 \leq H \leq 4$	1.7×10^9	408	1.7×10^9	2.8×10^9
$4 \leq H \leq 2.5$	2.4×10^9	528	2.4×10^9	3.6×10^9
$2.5 \leq H \leq 0$	3.3×10^9	600	3.0×10^9	4.1×10^9

Table VI. Support Tower, Air Fill

At the base of the tower, each cluster supports a load of about 8.3×10^8 N over an area of approximately 600 m². This results in a load of 1.4×10^6 N/m² or 200 psi. Concrete with this pressure loading is readily available for the final foundation.

4.0 Conclusion

The proof of concept system will be a 25 km tall sub-scale model of a fully operational first generation system. The proof of concept system will demonstrate the viability of an all electric first stage launch system. It will demonstrate the launch of a second stage suborbital launch vehicle with separation from an overcarriage and the mitigation of the shock wave in the ribbon produced during launch.

The proof of concept system will demonstrate torque buffering while restoring rotational kinetic energy and demonstrate gyroscopic and pressure stabilization of the unbalanced force. Finally, the proof of concept system will demonstrate the viability of using inflated multi-beams for heavy load bearing structures in the tall towers of the Space Track Launch System.

References

1. Fisher, J.F., 2011, *Space Track Launch System - Updated Oct, 2011*, www.fisherspacesystems.com/linked/stlsupdated10062011.pdf
2. Fisher, J.F., 2010, *Space Track Launch System – Counterweight*, www.fisherspacesystems.com/linked/stlscounterweight.pdf
3. Fisher, J.F., 2009, *Space Track Launch System - Second Stage Requirements*, www.fisherspacesystems.com/linked/stls2ndstagereq.pdf
4. Fisher, J.F., 2010, *Space Track Launch System – Overcarriage*, www.fisherspacesystems.com/linked/stlsovercarriage.pdf
5. Incropera, F.F. and DeWitt, D.P., 1985, *Introduction to Heat Transfer*, John Wiley & Sons, Inc.

Fisher Space Systems, LLC

6. FoilSim, 2012, <http://www.grc.nasa.gov/WWW/K-12/FoilSim/index.html>, accessed Jun 2012

Input parameters:

Plate

Camber = 0.0 % chord , Thickness = 1.0 % chord ,

Chord = 0.999 m , Span = 10.0 m ,

Surface Area = 10.0 sq m ,

Angle of attack = 1.0 degrees ,

Standard Earth Atmosphere

Altitude = 15087 m , Density = 0.19kg/cu m

Pressure = 11.833kPa, Temperature = -56C,

Airspeed = 396 km/hr ,

Lift Coefficient = 0.109

Drag Coefficient = 0.011

7. Carroll, J.A., 1985, "Guidebook for Analysis of Tether Applications", Joseph A. Carroll, Final Report on Contract RH4-394049 with the Martin Marietta Corporation, William Nobles, Technical Monitor, March 1985, p. 9

8. Kevlar, 2012, KEVLAR Technical Guide, Aramid Fiber, accessed Jun 2012
www2.dupont.com/Kevlar/en_US/assets/downloads/KEVLAR_Technical_Guide.pdf

9. Fox, R.W. and McDonald, A.T., 1992, *Introduction to Fluid Mechanics*, Fourth Edition, John Wiley & Sons, Inc., Eq A.1, p. 762, T = 217K

10. Incropera, F.F. and DeWitt, D.P., 1985, *Introduction to Heat Transfer*, John Wiley & Sons, Inc., Table A.4, p681

11. Fisher, J.F. , 2012, Space Track Launch System - Flexible Ribbon Model,
www.fisherspacesystems.com/linked/flexribmod.pdf

12. Rohrschneider, R.R., 2002, *Development of a Mass Estimating Relationship Database for Launch Vehicle Conceptual Design*, Georgia Institute of Technology, Under the Academic Supervision of Dr. Joohn R. Olds, AE 8900, April 26, 2002

13. Project Mercury, 1963, NASA-TM-X-51173, Project Mercury (MODM Project), Quarterly Status Report ending 31 Jan 1963

14. de Vries, J. 2006, *Space Elevator - Design Synthesis Exercise 2005*, Delft University of Technology, p. 44

15. M5[®], 2006, www.m5fiber.com/magellan

16. American Superconductor, 2010, *High Temperature Superconductor Ship Propulsion Motors*, www.amsc.com/pdf/MP_DS_365_0610.pdf

Fisher Space Systems, LLC

17. ECOA Industrial Products, Inc. 2004, Magnum™ ECOA Series MLTQD Scissor Lift Tables, www.ecoalifts.com/product/15.pdf

18. R.K. Seth, B.M. Quine, and Z.H. Zhu, 2009, "Feasibility of 20 Km Free-Standing Inflatable Space Tower" JBIS, Vol 62, pp. 342-353, 2009

19. Seth, 2010, Raj Kumar Seth, "On the Design and Feasibility of a Pneumatically Supported Actively Guided Space Tower", submitted to the faculty of graduate studies in partial fulfillment of the requirements for the degree of Doctor of Philosophy, Graduate Programme in Physics and Astronomy, York University, Toronto, Ontario, August 2010.